TIME-DEPENDENT DIFFUSION AND SURFACE RELAXATION IN RECONSTRUCTED POROUS ROCK

Sadiq Olayinka and Marios A. Ioannidis

Porous Media Research Institute,
Department of Chemical Engineering,
University of Waterloo, Waterloo, Ontario,
N2L 3G1, Canada.

ABSTRACT

Understanding the connection between pore structure and NMR behavior of fluid-saturated porous rock is essential in interpreting the results of NMR measurements in the field or laboratory and in establishing correlations between NMR parameters and petrophysical properties. Here, stochastic 3D replicas of real porous media, generated using low-order statistical information obtained from 2D images of the pore space, are used to study time-dependent diffusion and surface-enhanced relaxation. These processes are studied by means of random-walk simulation. A distinct advantage of using stochastic replicas of porous rock is that the geometric and topological properties of the pore space are known independently. Multiple 3D realizations of reservoir rock samples with different porosity and permeability are studied. In all cases, time-dependent magnetization is essentially bi-exponential and the short-T_2 value corresponds to the average surface-to-volume ratio. Similar pore size information is provided by analysis of time-dependent diffusion data at short times. A Padé approximant is used to interpolate between the short- and long-time diffusion data. Permeability estimates are obtained from pore sizes determined by multi-exponential inversion of simulated magnetization decays, as well as from geometric information extracted from diffusion simulations. These estimates are in close agreement with independently determined values.

INTRODUCTION

NMR relaxation methods have been widely used in the field and laboratory to characterize pore space geometry [1]. Additionally, pulsed-field-gradient (PFG) NMR experiments have enabled detailed measurements of molecular diffusion in restricted geometries, measurements that give microscopic, albeit volumetrically averaged, properties of the pore space [2]. To unravel the geometric information implicit in the results of these methods, one would like to perform the experiments in porous media with precisely known geometry. With the exception of bead packs and sinters, it is generally not possible to experiment with well-characterized porous media. Furthermore, NMR experiments are often subject to practical constraints, which limit the ranges of manipulated and measured variables. For these reasons, simulations have also been pursued, most of which have employed the random-walk method [3-6]. The model microstructures that have been thus investigated include simple geometric objects (spheres, slabs, etc.), ball-and-stick networks, packs of non-overlapping and overlapping

spherical particles of uniform size, and site-percolation lattices. To our knowledge, 3D models reconstructed by stochastic methods from image statistical information [7] have not been studied. This task is undertaken here. We expect that studies of NMR processes in realistically complex, yet well characterized microstructures, may lead to improvements in the interpretation of experimental results and may identify directions for further development of stochastic models of porous media.

The mean-squared displacement of fluid molecules undergoing unrestricted diffusion by random Brownian motion is given by

$$\left\langle [r(t)-r(0)]^2 \right\rangle = 6D_0 t \tag{1}$$

where $r(t)$ is the position of the molecule at any particular time t and D_0 is the bulk diffusivity of the fluid. Solid walls restrict diffusion of the molecules within the pore space and the mean squared displacement $\left\langle [r(t)-r(0)]^2 \right\rangle$ is reduced from $6D_0 t$. This is often expressed as an effective diffusion coefficient $D(t)$ [4]:

$$D(t) = \frac{1}{6t}\left\langle [r(t)-r(0)]^2 \right\rangle \tag{2}$$

At short times, only a surface layer of diffusing particles near the pore walls feels the effects of restricted diffusion and $D(t)$ varies as [8]:

$$\frac{D(t)}{D_0} = 1 - \frac{4S}{9V_p\sqrt{\pi}}\sqrt{D_0 t} + O(D_0 t) \tag{3}$$

where S/V_p is the average pore surface-to-volume ratio. Thus, PFG-NMR offers a means to determine S/V_p without reference to the surface relaxivity ρ. In conjunction with relaxation measurements, this enables the determination of ρ. At long times, the reduced diffusion coefficient is expected to vary as:

$$\lim_{t\to\infty}\frac{D(t)}{D_0} = \frac{1}{F\phi} \equiv \frac{1}{\tau} \tag{4}$$

where τ is the tortuosity. The following formula has been widely used for interpolating between the short- and long–time limits [9]:

$$\frac{D(t)}{D_0} = 1 - \left(1-\frac{1}{\alpha}\right)\times\frac{c\sqrt{t}+(1-1/\alpha)t/\theta}{(1-1/\alpha)+c\sqrt{t}+(1-1/\alpha)t/\theta} \tag{5}$$

where $c = (4/9\sqrt{\pi})(S/V_p)\sqrt{D_o}$, $1/\alpha = \lim_{t\to\infty} D(t)/D_0$ and θ has dimensions of time.

It has been suggested that, in the presence of surface relaxation, $1/\alpha$ is different from $1/\tau$ [10]. Simulations with ordered cubic and random packings of monosized spheres have shown $1/\alpha < 1/\tau$ [4]. However, experiments in random monosized sphere packs have yielded $1/\alpha = 1/\tau$ [9,12]. Experiments in real rock with water as the probe molecule have some times suggested $1/\alpha > 1/\tau$ [11] and some times suggested $1/\alpha = 1/\tau$ [13].

Experiments in real rock with polarized xenon gas as the probe molecule have shown $1/\alpha = 1/\tau$ [12]. In random monosized bead packs, $\sqrt{D_0\theta}$ is experimentally shown to be equal to $d/6$, the inverse surface-to-volume ratio of a sphere of diameter *d* [9]. This is so because in such simple structures, the bead diameter controls the average pore surface-to-volume ratio. This result is unlikely to hold for porous media possessing an irregular rock-pore interface. Hurlimann *et al*. [11] analyzed PFG-NMR data for rocks using Eq. (5) by assuming $1/\alpha = 1/\tau$. They found values of $\sqrt{D_0\theta}$ well in excess of the average V_p/S, in contradiction with the theory behind Eq. (3). In summary, there appears to be considerable uncertainty regarding the nature of geometric information that may be extracted from PFG-NMR experiments.

SIMULATION PROCEDURES

Description of the Random Walk Algorithm

The porous media studied have been described in detail elsewhere [7]. Each medium is represented as a 3D array of 256^3 solid and void voxels of size ε. We use a discrete random walk algorithm following the formulation of Wilkinson *et al*. [5] for calculating the random walk parameters. Initially, each walker is placed in the center of a randomly chosen void voxel. At any instance during its lifetime, the void voxel in which the walker resides is discretized into N^3 subvoxels, where $N = \varepsilon/p$ and p is the step of the random walk. The walker is then allowed to take random steps along any orthogonal or diagonal direction and time is incremented. A walker that reaches the boundary of its containing void voxel may, in a subsequent step, move to a neighboring solid or void voxel. If the neighboring voxel is void, the random walker continues moving and time is incremented. If, however, the neighboring voxel is solid, then the walker is extinguished with a probability the magnitude of which depends on the surface relaxivity ρ [5] and time is incremented. A total of M_0 walkers are released and the number of survivors after time *t*, $M(t)$, as well as their squared displacements are recorded. From these data, the relaxation function is calculated as

$$g(t) = M(t)/M_0 \tag{6}$$

and the time dependent diffusion is calculated as

$$D(t) = \frac{1}{6M(t)t}\sum_{n=1}^{M(t)}\left[r_n(t) - r_n(0)\right]^2. \tag{7}$$

We analyze the simulated relaxation function $g(t)$ in terms of a multiexponential model:

$$M(t) = M_o\sum_i f_i \exp(-t/T_i) \tag{8}$$

and relate characteristic pore sizes, $(V_p/S)_i$, to relaxation times, T_i, as follows:

$$\frac{1}{T_i} = \rho\left(\frac{S}{V_p}\right)_i. \tag{9}$$

Verification of Random Walk Algorithm

We verified the algorithm using a spatially periodic microstructure comprised of identical cubic pores of side length $L = 4\,\mu m$, resolved in computer memory by voxels of side length $\varepsilon = 1\,\mu m$, and communicating through rectangular openings (pore throats) of size equal to one voxel ("swiss-cheese" model). This microstructure has $\langle S/V_p \rangle = 9/7$ μm^{-1}. We found that for $N < 64$ the results depended on the step size of the random walk and selected to work with $N = 81$. Figure 1A shows excellent agreement between the simulated $g(t)$ (points) and the theoretical result $\exp(-9\rho t/7)$ (lines) for three different values of ρ. Figure 1B shows that for this microstructure, (i) the long-time limit of time-dependent diffusion coefficient is independent of the strength of surface relaxation ($1/\alpha = 1/\tau$) and, (ii) Eq. (3) with $\langle S/V_p \rangle = 9/7$ μm^{-1} describes the early-time behavior, as expected.

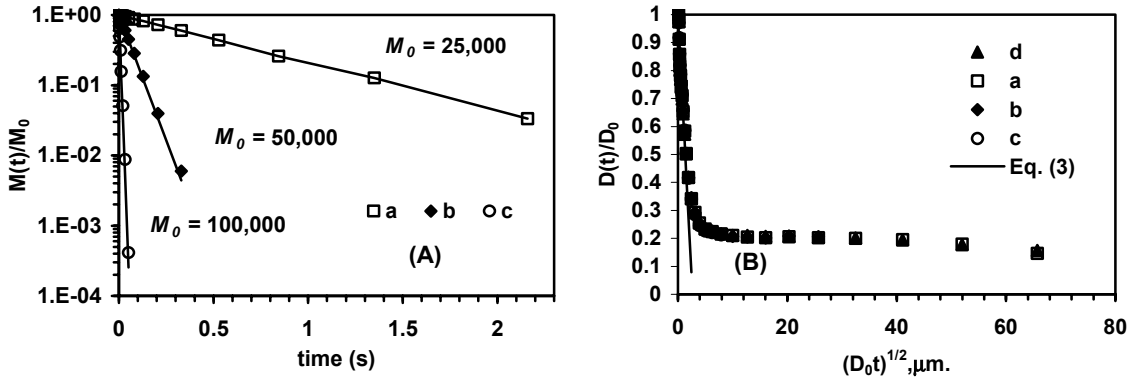

Figure 1: Algorithm verification simulations in "swiss-cheese" model: (A) Magnetization decay; (B) Time-dependent diffusion. In these figures (a) ρ=1.28 $\mu m/s$, (b) ρ=12.8 $\mu m/s$, (c) ρ=128 $\mu m/s$ and (d) ρ=0 $\mu m/s$. In all simulations $D_0 = 2.5\times10^{-9}$ m^2/s.

RESULTS AND DISCUSSION

The microstructure of 3D stochastically reconstructed porous media is controlled by their porosity ϕ and autocorrelation function $R_z(r)$ [7]. Two length scales are immediately distinguished. The first one is the integral correlation length λ, a length scale representative of the average pore size [14,15]:

$$\lambda = \int_0^\infty R_z(r)dr\,. \tag{10}$$

The second one is the length scale describing surface asperity, which in reconstructed porous media corresponds to the size ε of one voxel. The correlation length λ is fairly insensitive to the resolution ε with which the pore space is represented [15], but ε largely

controls the average pore surface-to-volume ratio $\left\langle S/V_p \right\rangle$. The latter is also related to the slope of the autocorrelation function at the origin:

$$\left\langle \frac{S}{V_p} \right\rangle = -6(1-\phi)\left.\frac{dR_z}{dr}\right|_{r=0}. \qquad (11)$$

For the five media studied, $1.05 \le \varepsilon \le 6.26$ μm, $0.94 \le \left\langle S/V_p \right\rangle^{-1} \le 6.17$ μm, $7.6 \le \lambda \le 59.9$ μm and $0.126 \le \phi \le 0.198$ (see also Table 1).

Results of random walk simulations for two different values of ρ (1.28 and 12.8 μm/s) are collected in Figure 2. As shown in Figure 2A and Figure 2D, the decay of magnetization increases as ρ increases and as the correlation length (average pore size) decreases. Both trends are expected. At early times, we also expect the reduced diffusion coefficient to be dependent only on $\left\langle S/V_p \right\rangle$ and independent of ρ. This is indeed the case as shown in Figure 2B and Figure 2E: regardless of the value of ρ, the early-time diffusion data for different media collapse into a single curve when the diffusion length is scaled by $\left\langle S/V_p \right\rangle$. The short-time regime persists until the diffusion length is approximately equal to $\left\langle V_p/S \right\rangle$, that is for length scales of the order of surface roughness ε. These results are also in accord with theory. At longer times the effects of correlation length and surface relaxation strength become apparent (see Figure 2C and Figure 2F). The effective diffusivity is seen to increase from a minimum value reached when $\sqrt{D_0 t} \approx \left\langle S/V_p \right\rangle^{-1}$ to a maximum value that increases with increasing ρ and increasing λ. This non-monotonic behavior of effective diffusivity may be explained as follows. At short times, obstacles of size ε restrict the diffusion of molecules near the pore surface and within the smallest pores (pores of size ε), whereas diffusion of molecules in larger pore spaces is unrestricted. At longer times, many of these molecules are extinguished on the surface, ceasing to contribute small displacements to the average in Eq. (7), and the effective diffusivity increases. The effective diffusivity recovers more readily when ρ is increased because an increase in surface relaxation reduces diffusive coupling between pores of different sizes (size ε and size λ). When the molecules have diffused distances of the order 10-20ε (a few correlation lengths in the media studied), they encounter obstacles of size λ and the effective diffusivity begins to slowly decrease.

The behavior described above is not observed in the simple "swiss-cheese" microstructure (see Figure 1B) in which relaxation is mono-exponential. It also not observed in simulations in sphere packs [4,9,12]. Both of these microstructures lack the irregular rock-pore interface and broad pore size distributions that characterize natural rock. Our simulations are, however, in qualitative agreement with recent experiments of gas diffusion NMR on Fontainebleau sandstone and Indiana limestone [12].

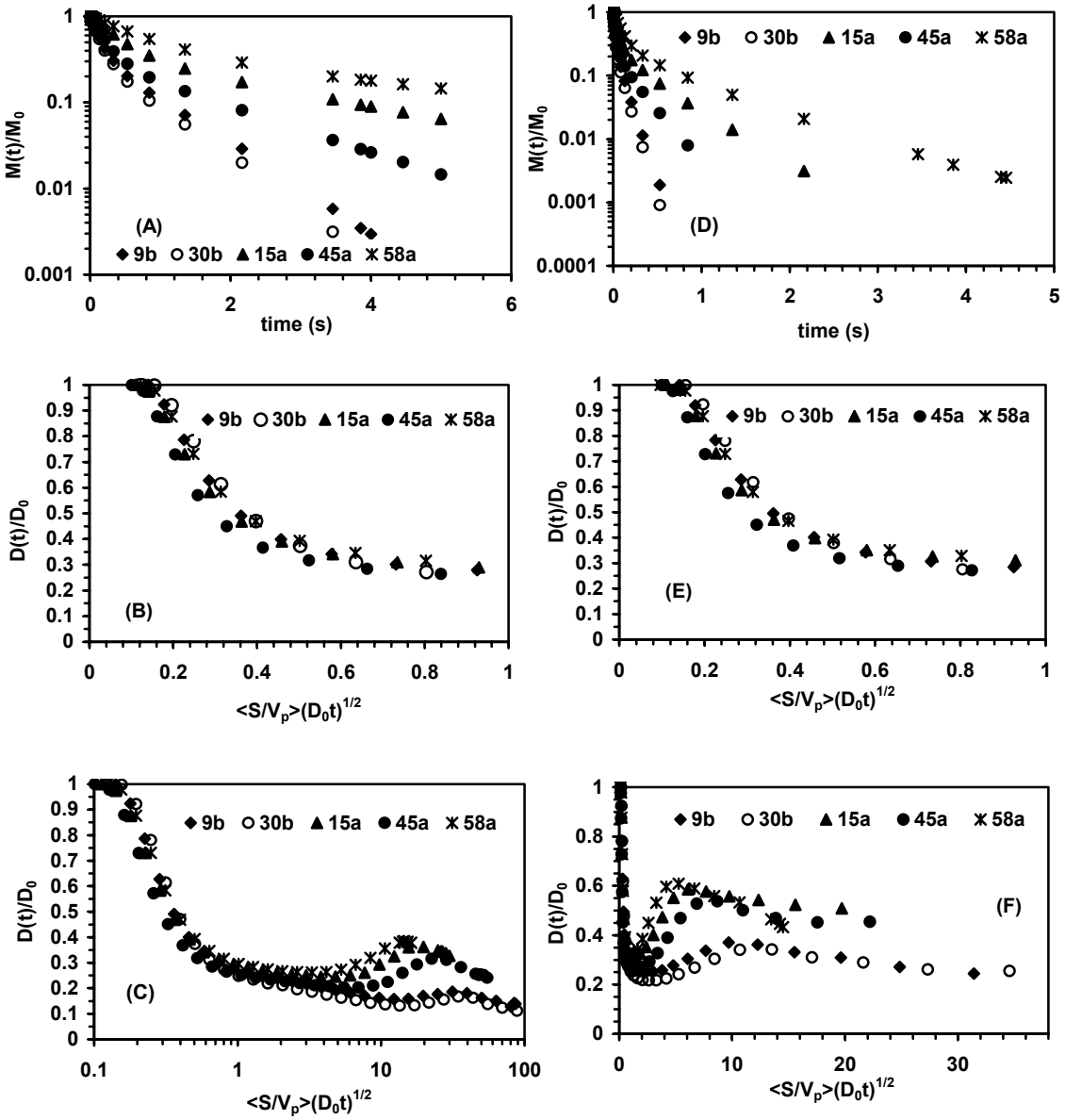

Figure 2: Results of random walk simulations in stochastically reconstructed porous media. Magnetization decay (panels A & D). Time-dependent diffusion coefficient, short-time data (panels B & E). Time-dependent diffusion coefficient, all data (panels C & F). Simulations for $\rho = 1.28\,\mu m/s$ (panels A, B & C) and $\rho = 12.8\,\mu m/s$ (panels D, E & F). Diffusion length normalized by $\langle S/V_p \rangle$ (determined directly by voxel counting).

Table 1. Geometric properties of stochastic media from analysis of time-dependent diffusion data.

Sample	ϕ	λ (μm)	ε (μm)	$\left\langle \frac{S}{V_p} \right\rangle$ $(\mu m)^{-1}$	$1/\alpha$		$\sqrt{D_0\theta}$ (μm)		$1/\tau$
					$\rho =$ 1.28 $\mu m/s$	$\rho =$ 12.8 $\mu m/s$	$\rho =$ 1.28 $\mu m/s$	$\rho =$ 12.8 $\mu m/s$	
9B	0.155	7.6	1.05	0.967	0.186	0.210	0.33	0.32	0.08
15A	0.170	36.6	3.08	0.300	0.208	0.208	0.97	1.02	0.11
30B	0.126	7.6	1.05	1.064	0.153	0.171	0.34	0.33	0.06
45A	0.148	23.6	1.54	0.548	0.197	0.175	0.48	0.51	0.10
58A	0.198	59.9	6.26	0.162	0.300	0.187	1.97	2.10	0.13

With prior knowledge of the intrinsic pore surface-to-volume ratio, we used the two-point Padé approximant, Eq. (5), to fit the reduced diffusion coefficient data. Only data corresponding to monotonic decrease of reduced diffusivity with time were used in the fitting. The best-fit values of $\sqrt{D_0\theta}$ and $1/\alpha$ for surface relaxivity values of 1.28 $\mu m/s$ and 12.8 $\mu m/s$ are reported in Table 1. The electrical tortuosity limits, $1/\tau$, obtained from simulations with $\rho = 0\,\mu m/s$ are also provided for comparison. Typical results are plotted in Figure 3. We observed that setting $1/\alpha = 1/\tau$ as an additional constraint in the fits did not change the best-fit values of $\sqrt{D_0\theta}$. Table 1 shows that the values of $\sqrt{D_0\theta}$

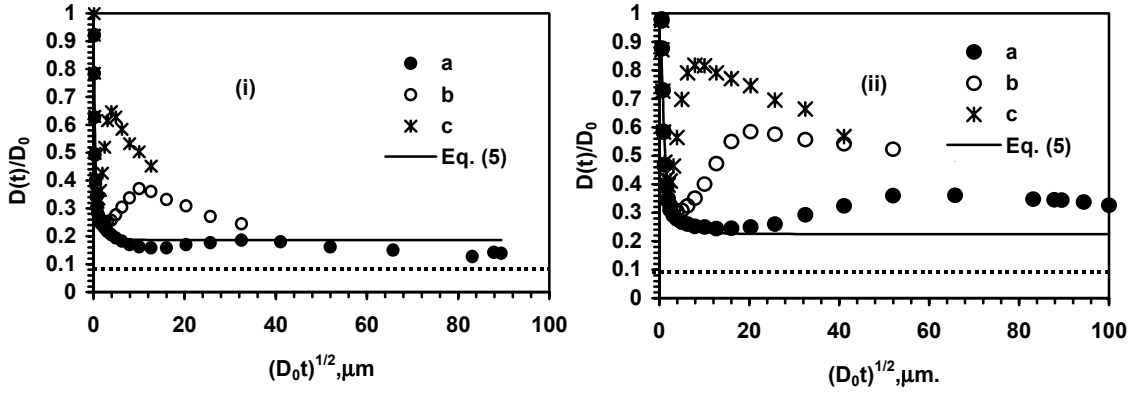

Figure 3. Padé fits to time-dependent diffusion data for sample 9B (i) and 15A (ii). In these figures (a) $\rho = 1.28\,\mu m/s$, (b) $\rho = 12.8\,\mu m/s$ and (c) $\rho = 128\,\mu m/s$. Dotted line corresponds to $1/\tau$.

are robust with respect to changes in surface relaxivity. As expected by theory, these values are smaller than $\langle S/V_p \rangle^{-1}$, by approximately a factor of three in all cases. Equation (5) fits all the data very well at early times, but it generally reaches an asymptotic value higher than $1/F\phi$ - the value obtained in the absence of surface relaxation. This results in underestimation of the formation factor by a factor that varies from 2 to 3. It is therefore not possible to obtain $1/\tau$ by extrapolation of the early-time data. It appears that molecules must diffuse several multiples of the correlation length scale before the long-time limit $1/\tau$ is reached. In Figure 3(i), the longest distance traveled by diffusing molecules is about 38 μm or 5 correlation lengths, whereas in Figure 3(ii) it is only 55 μm or 1.5 correlation length. Such distances are apparently insufficient to reach the tortuosity limit.

Multiexponential inversion of the simulated magnetization decays reveals that relaxation is essentially bi-exponential. Typical results are shown in Figure 4. In all cases, a considerable fraction of the pore space is associated with a relaxation rate that corresponds to $S/V_p = 6/\varepsilon$, that is cubic pores of size ε. The results highlight the effect

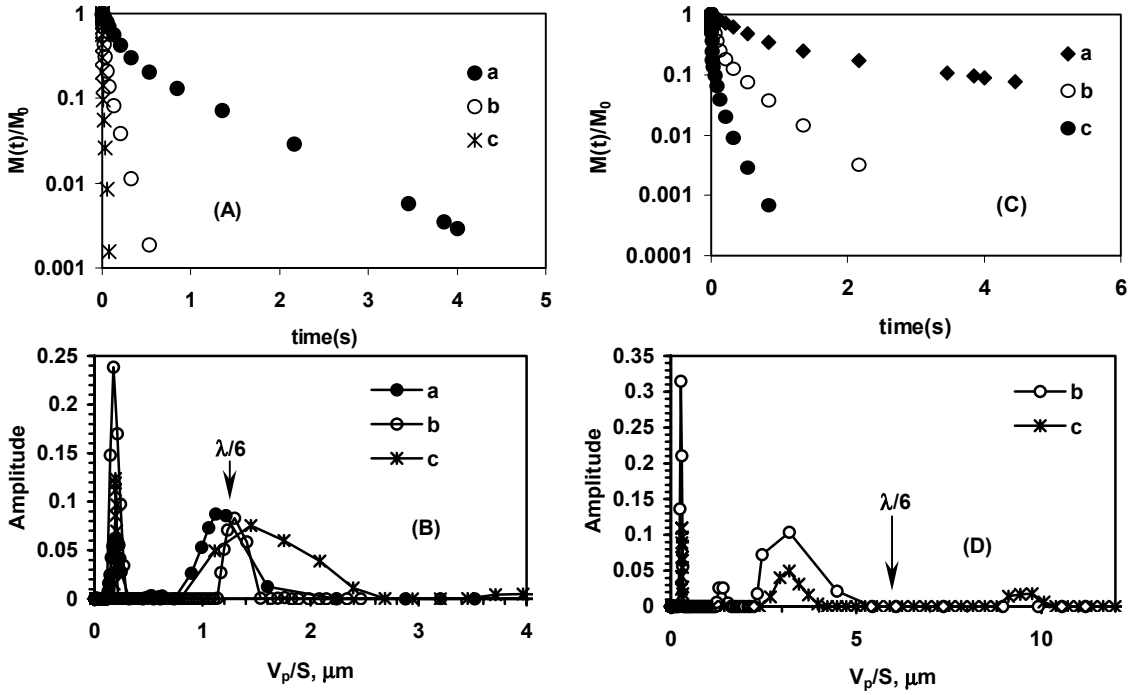

Figure 4: Magnetization decay (panels A & C) and corresponding pore size distribution (panels B & D) for samples 9B (panels A & B) and 15A (panels C & D). Results for different surface relaxivity values: (a) $\rho = 1.28\,\mu m/s$, (b) $\rho = 12.8\,\mu m/s$ and (c) $\rho = 128\,\mu m/s$.

of diffusional coupling - NMR-derived pore size distributions do not correspond exactly to pore size distributions obtained by pore space partitioning [14] because molecular diffusion averages magnetization over regions that extend beyond the geometric boundaries of individual pores. Nonetheless, the main geometric features are recovered: the average relaxation time - excluding relaxation times associated with pores of size ε - is identified with $V_p/S = \lambda/6$. At this point it is instructive to recall the results of earlier simulations of relaxation on site-percolation lattices [3]. The key difference between a site-percolation lattice and the microstructures investigated here is due to the correlation $R_z(r)$: in a site-percolation lattice $\lambda \approx \varepsilon$. It is therefore not surprising that mono-exponential relaxation was observed in site-percolation lattices [3], for such media do not contain disparate length scales. Scale separation is not great in the media considered here - λ/ε varies from 7 to 15 (see Table 1) - and this is one of the reasons magnetization decay is not governed by a broad distribution of relaxation times. In fact, it has been directly demonstrated that the breadth of pore size distributions in stochastically reconstructed porous media increases with increasing λ/ε [14]. The other reason is averaging of magnetization by diffusion, as already mentioned. Finally, it is important to note that, while λ can be determined experimentally with good accuracy, *e.g.* from backscatter scanning electron micrographs [15], ε is resolution-dependent. Since sedimentary rocks are extensive surface fractals [16], it is likely that in reality $\lambda/\varepsilon = O(10^4)$. At present, however, three-dimensional computer reconstruction of porous media is limited to $\lambda/\varepsilon < 20$.

Having established that the main geometric features of the microstructures investigated are reflected in both NMR diffusion and relaxation data, we examined whether it is possible to use this information to predict their permeability. Empirically we know that permeability correlates with ϕ and λ [15]. Since the latter length scale is reflected in the average relaxation time $\langle T \rangle$ - excluding relaxation times associated with pores of size ε ("microporosity") - it is natural to test the predictor $k'' \propto \phi^4 \langle T \rangle^2$. An alternative expression is derived from the following formula proposed for our stochastic media [7]:

$$k' = \frac{64}{226F} \left\langle \frac{S}{V_p} \right\rangle^{-2} \tag{12}$$

where here we assumed $F \approx \alpha/\phi$ in order to test this expression with NMR diffusion data ($\langle S/V_p \rangle, 1/\alpha$). The results of the calculations for different values of the surface relaxivity are compared to numerically computed permeability values (k_{calc}, [7]) in Table 2, where $\langle S/V_p \rangle_{<T>}$ is the pore surface-to-volume ratio associated with $\langle T \rangle$ via Eq. (9). The values of the prefactor in the permeability predictor $k'' \propto \phi^4 \langle T \rangle^2$ are

$1\times10^{6}\,s^{-2}$ and $2\times10^{7}\,s^{-2}$ for ρ values of $12.8\,\mu m/s$ and $128\,\mu m/s$, respectively, with T in seconds. It is observed that both predictors do a good job in explaining permeability. Equation (5) provides a long time limit, $1/\alpha$, which can be used to explain permeability according to Eq. (12) for surface relaxivity values of $1.28\,\mu m/s$ and $12.8\,\mu m/s$. Magnetization data at ρ values of $12.8\,\mu m/s$ and $128\,\mu m/s$ also provide a good prediction of permeability. This might seem surprising, for the two predictors make use of different characteristic length scales, λ and ε. The explanation lies in the nearly constant ratio λ/ε for these media. Physically, stochastic replicas of rock samples with large average pore size (large λ, *e.g.*, samples 58A and 15A) have relatively low resolution. A coarser description is tantamount to smoothing, such that $\langle S/V_p \rangle$ in Eq. (12) - and all Kozeny-based formulas for that matter - is the average surface-to-volume ratio of the main flow pathways, that is the pore channels which are invaded by a non-wetting phase at the percolation threshold. Indeed, this has been directly verified [7].

Table 2. Predictions of the permeability of stochastic media from NMR data

Sample	ϕ	$\langle T \rangle$ (s)		$\langle S/V_p \rangle_{<T>}$ $(\mu m)^{-1}$		k_{calc} (mD)	k' (mD)		k'' (mD)	
		B	C	B	C		A	B	B	C
9B	0.155	0.010	0.031	0.785	0.253	4.19	8.62	9.72	5.66	10.9
15A	0.170	0.380	0.085	0.205	0.092	169.	119.	110.	128	129.
30B	0.126	0.090	0.012	0.864	0.647	1.60	4.75	5.33	2.11	0.75
45A	0.148	0.235	0.074	0.332	0.105	24.4	27.1	24.1	19.8	39.8
58A	0.198	0.716	0.207	0.109	0.038	744.	484	395	781	1310.

A: $\rho=1.28\,\mu m/s$; B: $\rho=12.8\,\mu m/s$; C: $\rho=128\,\mu m/s$

CONCLUSIONS

A random walk algorithm was used to simulate the NMR processes of time-dependent diffusion and surface-enhanced relaxation in 3D reconstructed porous media. The simulations provided new insights in the properties of an important class of porous media models. In accordance with theoretical expectations, it was found that magnetization decays faster in stochastic media characterized by small correlation length, λ, and high average surface-to-volume ratio, $\langle S/V_p \rangle$. In all cases, magnetization decays were essentially bi-exponential and the corresponding pore size distributions distinctively bimodal. NMR-derived pore size distributions were shown to be considerably affected by diffusion. The mode corresponding to the shortest relaxation times was clearly associated with values of S/V_p characteristic of pore surface roughness. The mode

corresponding to the longest relaxation times was associated with values of S/V_p characteristic of the pore size controlling the permeability of the stochastic media. Simulations of restricted diffusion were in agreement with theoretical expectations, in that surface relaxation does not affect the short time behavior. Instead, at early times, the reduction of effective diffusivity is solely controlled by the average pore surface-to-volume ratio. The simulations also revealed that the effective diffusivity is not a monotonically decreasing function of time. This is contrary to the results of simulations in simple geometries (*e.g.*, aggregates of identical spheres), but agrees with experimental observations in real media. Additionally, the long-time limit of the reduced diffusion coefficient in the presence of surface relaxation was shown to underestimate the true tortuosity. This finding is also contrary to the results of simulations in bead packs and in agreement with experiments in real rock. Finally, it was shown that the permeability of stochastically generated porous media could be predicted from NMR parameters. These findings provide support for the use of 3D stochastic models of porous rock and assist in the interpretation of experimental NMR data.

REFERENCES

1. Kenyon, W.E., "Petrophysical Principles of Applications of NMR Logging", *The log analyst*, (1986) **34**, 11, 8179.
2. Stallmach, F. and J. Kärger, "The Potential of Pulsed Field Gradient NMR for Investigation of Porous Media", *Adsorption*, (1999) **5**, 117-133.
3. Mendelson, K.S., "Percolation Model of Nuclear Magnetic Relaxation in Porous Media", *Physical Review B*, (1990) **44**, 1, 562-567.
4. Sen, P.N., L.M. Schwartz, P.P. Mitra and B.I. Halperin, "Surface Relaxation and Long-time Diffusion Coefficient in Porous Media: Periodic Geometries", *Physical Review B*, (1994) **49**, 1, 215-225.
5. Wilkinson, D.J, D.L. Johnson and L.M. Schwartz, "Nuclear Magnetic Relaxation in Porous Media: The Role of the Mean Lifetime $\tau(\rho$, D)", *Physical Review B*, (1991) **44**, 10, 4960-4973.
6. Bergman, D.J, K.J. Dunn, L.M. Schwartz and P.P. Mitra, "Self-Diffusion in a Periodic Porous Medium: A Comparison of Different Approaches", *Physical Review E*, (1995) **51**, 4, 3393-3400.
7. Liang, Z., M.A. Ioannidis and I. Chatzis, "Permeability and electrical conductivity of porous media from 3D stochastic replicas of the microstructure", *Chemical Engineering Science*, (2000) **55**, 5247-5262.
8. Mitra, P.P, P.N. Sen, L.M. Schwartz and P.L. Doussal, "Diffusion Propagator as a Probe of the Structure of Porous Media", *Physical Review Letters*, (1992) **68**, 24, 3555-3558.
9. Latour, L.L., P.P. Mitra, R.L. Kleinberg and C.H. Sotak, "Time-Dependent Diffusion Coefficient of Fluids in Porous Media as a Probe of Surface-to-Volume Ratio", *Journal of Magnetic Resonance*, (1993) Series A 101, 342-346.

10. Schwartz, L.M., P.N. Sen and P.P. Mitra "Simulations of Pulsed Field Gradient Spin-Echo Measurements in Porous Media", *Magnetic Resonance Imaging*, (1994) **12**, 2, 241-244.
11. Hürlimann, M.D., K.G. Helmer, L.L. Latour and C.H. Sotak, "Restricted Diffusion in Sedimentary Rocks. Determination of Surface-Area-to-Volume Ratio and Surface Relaxivity", *Journal of Magnetic Resonance*, (1994) Series A 111, 169-178.
12. Mair, R.W., G.P. Wong, D. Hoffmann, M.D. Hürlimann, S. Patz, L.M. Schwartz and R.L. Walsworth, "Probing Porous Media with Gas Diffusion NMR*", Physical Review Letters*, (1999) **83**, 16, 3324-3327.
13. Frosch, G.P., J.E. Tillich, R. Haselmeier, M. Holz and E. Althaus, "Probing the Pore Space of Geothermal Reservoir Sandstones by Nuclear Magnetic Resonance", *Geothermics*, (2000) **29**, 671-687.
14. Ioannidis, M.A. and I. Chatzis, "On the Geometry and Topology of 3D Stochastic Porous Media", *Journal of Colloid & Interface Science*, (2000) **229**, 323-334.
15. Ioannidis, M.A., M.J. Kwiecien and I. Chatzis, "Statistical analysis of the porous microstructure as a method for estimating reservoir permeability", *Journal of Petroleum Science and Engineering*, (1996) **16**, 251-261.
16. Radlinski, A.P., M.A. Ioannidis, A.L. Hinde, M. Hainbuchner, M. Baron, H. Rauch, and S.R. Kline, "Multiscale Characterization of Reservoir Rock Microstructure: Combining Small-Angle Neutron Scattering and Image Analysis", to appear in the Proceedings of the Annual Symposium of the Society of Core Analysts, Monterey, California, September 2002.